

# Cyclic resistance and shear stiffness properties of a clean sand stabilized with colloidal silica

A.D. Vranna\* and Th. Tika

*Aristotle University of Thessaloniki, Thessaloniki, Greece*

*\*Corresponding Author*

**ABSTRACT** This paper presents results from a laboratory investigation into passive site stabilization of liquefiable sands by injecting colloidal silica (CS). In order to examine the improvement of the cyclic resistance and shear stiffness of liquefiable sands stabilized with CS, cyclic triaxial and bender element tests were performed on a clean quartz sand stabilized with two different concentrations of CS. The stabilized sample preparation method adopted in the tests is initially described and then results from the above tests conducted on treated and untreated samples are presented. It is shown that stabilization of the sand with CS significantly improves the cyclic resistance, as well as the shear stiffness. Whereas the increase in CS concentration does not influence the cyclic resistance of the stabilized sand, it results in the increase of shear stiffness.

## 1 INTRODUCTION

Liquefaction of sandy soils is one of the major causes of damage of earth structures and foundations during earthquakes. Over the last decades, widespread liquefaction-induced ground deformation and related damage to foundations has occurred, as a result of urban expansion and building on liquefaction-prone sites. Thus mitigation and preventing damage, due to liquefaction under existing developed sites, is one of main issues of seismic design. To this end, the technique of passive site stabilization of liquefiable soil under existing structures has been proposed (Gallagher & Mitchell 2002). This method is based on the use of nanomaterials, such as colloidal silica, laponite and bentonite, and involves slow injection of the stabilization nanomaterial into the liquefiable soil by means of natural or augmented groundwater flow.

Colloidal silica (CS) is an aqueous suspension of microscopic silica particles, produced from saturated solutions of silicic acid,  $H_4SiO_4$  (Iler 1979). In dilute solutions, CS has a density and viscosity similar to

those of water and can be made to gel by adjusting the ionic strength or pH of a given CS solution. This property allows it to be injected or mixed with soil, so that after gelling colloidal silica blocks the void space in the soil and therefore alters its mechanical behaviour. The principal advantages of CS over other potential stabilizers are its excellent durability characteristics, its initial low viscosity and the ability to attain low permeability in grouted soils, long controllable and reproducible gel times, non-toxicity and low cost.

Previous research on the mechanical behaviour of sands stabilized with CS mainly involved unconfined compressive strength tests and physical modelling tests. Monotonic and cyclic triaxial testing on sands stabilized with CS are reported in literature among a few others by Kabashima & Towhata (2000), Gallagher & Mitchell (2002), Díaz-Rodríguez et al. (2008) and Mollamahmutoglu & Yilmaz (2010). Reported studies concerning the shear stiffness of sands stabilized with CS are even more limited and have

been mainly conducted by means of resonant column and centrifuge model tests.

With increasing application of passive site stabilization, however, there is need to better understand both the strength and stiffness characteristics of liquefiable sands that are stabilized with CS under different loading conditions, as well as to assess the limits of the applicability of this improvement method. Vrana & Tika (2015) investigated the monotonic and cyclic behaviour of a clean sand stabilized with CS with 10% concentration and the work presented herein is an extension to the above work. To this end, a series of cyclic and bender element tests was performed on a clean quartz sand, stabilized with two different CS concentrations, of 6% and 10%. The effectiveness of the CS stabilization was investigated by conducting also a series of cyclic and bender element tests on untreated sand samples. The results from the two series of tests are presented and discussed.

## 2 EXPERIMENTAL PROCEDURE

### 2.1 Tested materials

The soil used in this study is a natural clean quartz sand (M31) with grains of variable roundness and sphericity. It has a specific gravity  $G_s = 2.655$ , maximum and minimum void ratios of  $e_{max} = 0.805$  and  $e_{min} = 0.558$  respectively, a mean diameter  $D_{50} = 0.31\text{mm}$  and a uniformity coefficient of  $C_u = 1.5$ . Its gradation curve lies within the bound gradation curves, suggested for liquefiable soils.

Ludox SM-30 was selected as the stabilizing agent of sand samples, supplied as a 30% by weight silica solution with a viscosity of 5.5cP, a pH of 10 and an average particle size of 7nm. Distilled water was added to the initial solution in order to obtain concentrations of 6% and 10% CS. Gel times of the two studied solutions were investigated by conducting viscosity measurement tests, by means of a rotating Brookfield viscometer (Vrana & Tika 2015). It is noted that gel time was defined as the elapsed time for which the tested solution viscosity is equal to  $\eta = 3.5\text{cP}$ . Beyond that value, viscosity increases rapidly and eventually the solution transforms into a rigid gel.

It was decided to employ CS gel times equal to 10 and 11 hours for the 10% and 6% CS solution, respectively. These times were achieved by adjusting the pH value to  $\text{pH} = 6.0$ , as well as the appropriate NaCl concentration of each solution.

### 2.2 Testing programme

The testing programme consisted of undrained isotropically consolidated cyclic triaxial tests on untreated, as well as CS treated sand samples. All tests were performed using a closed-loop automatic cyclic triaxial apparatus (M.T.S. Systems Corporation), equipped with bender elements.

Cylindrical samples (height/diameter  $\approx 100\text{mm} / 50\text{mm}$ ) were prepared at various densities, using the undercompaction method, as proposed by Ladd (1978), both for the untreated and treated sand. Saturation was achieved by percolating throughout the sample, first carbon dioxide gas ( $\text{CO}_2$ ) and then de-aired water. The CS solution was then injected into the samples until it filled the soil voids. The replacement of water by the CS solution was considered to be complete when a solution volume equal to four times the soil sample volume was extracted from the top of the sample. The viscosity of the CS solution remained low ( $\eta < 3.5\text{cP}$ ) throughout the sample percolation process.

After the setting of CS, treated samples were placed in a constant temperature and humidity chamber for a curing time of five times the CS gel time. Saturation of treated samples prior to testing was not performed, due to the infilling of pore spaces with CS and the possibility of damaging the formed CS bonds. It was assumed, therefore, that total confining,  $p_0$ , and effective confining,  $p'_0$ , stresses, coincide.

All samples were isotropically consolidated under  $p'_0$  ranging from 20 to 600kPa.

During cyclic loading, a sinusoidally varying axial stress ( $\pm\sigma_d$ ) was applied at a frequency of  $f = 0.1\text{Hz}$ , under undrained conditions. In this work, the occurrence of double amplitude axial strain,  $\varepsilon_{DA} = 5\%$  is used as a reference point to define cyclic softening of both treated and untreated samples. For this reason, a series of cyclic triaxial tests with different cyclic stress ratios,  $\text{CSR} = \sigma_d / 2p'_0$ , was carried out in order to determine the number of load cycles,  $N$ , required for the development of  $\varepsilon_{DA} = 5\%$  both for the treated and untreated samples. In view of the typical number

of load cycles of actual earthquakes (10 to 20 for an earthquake of M7.5 magnitude), the onset of cyclic softening and thus the cyclic resistance ratio,  $CRR_{15}$ , is considered as the CSR required to produce  $\varepsilon_{DA} = 5\%$  in 15 loading cycles. In this work, cyclic loading of the samples was conducted at  $p'_0 = 100\text{kPa}$ .

The bender elements were installed in specially constructed top and bottom platens of the cylindrical sample. A function generator was used for the excitation of the source element (top platen) with an electrical signal. A digital oscilloscope was used for the display and recording of both the input-source and output-receiver signals. The function generator and the oscilloscope were connected to a computer. The type of electrical signal used to drive the source element was a sinusoidal pulse of 10Volts (amplitude) at a frequency ranging from 3 to 10kHz. An automated measurements system was developed for signal acquisition and analyses which included recording, appropriate filtering and automated measurement of travel time of the signal in time and frequency domain (Theopoulos 2009).

The shear waves travel time through the samples was determined using the start-to-start (Kawaguchi et al. 2001) and cross correlation (Mancuso et al. 1989) methods, respectively. To account for the near field effect disturbances, due to the arrival of P waves before shear waves at the receiver element, as well as signal noises, signal arrival was observed by passing waves of different frequencies (Brignoli et al. 1996). According to the start-to-start method, when the first amplitude in the time history of the receiver signal matches the direction of source signal, the point where the receiver signal takes-off from the base line (horizontal line of zero voltage when there is no signal) is the time of shear wave arrival. In case the first amplitude in the time history of the receiver signal does not match the direction of source signal, the point where the receiver signal first transverses towards the source signal direction and intersects the base line, is the time of shear waves arrival. According to the cross correlation method, the arrival of shear waves at the receiver element is identified by the maximum of the cross-correlation function of the source and receiver signals.

For the untreated samples, the shear waves travel times determined by the start-to-start and cross-correlation methods, were practically identical. How-

ever, for the treated samples, problems were encountered in determining the shear waves travel time, using the start-to-start method. Due to this uncertainty, the cross correlation method was used for the estimation of the travel time for both types of samples. Measurements of shear wave velocity,  $V_s$ , were conducted after completion of consolidation and prior to cyclic loading.

### 3 TEST RESULTS AND ANALYSIS

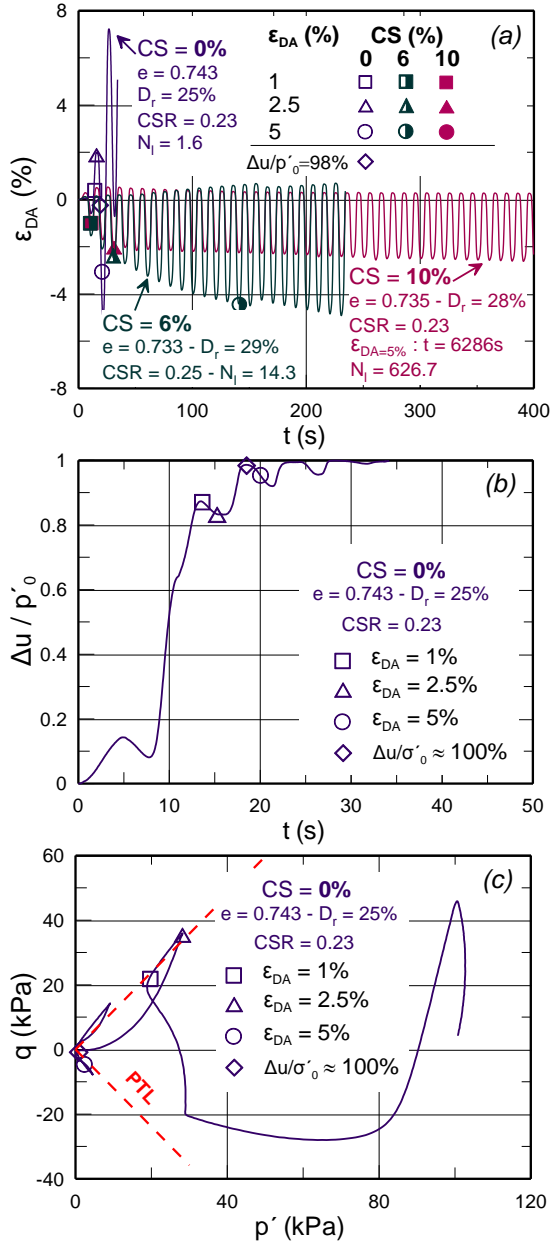
#### 3.1 Cyclic resistance

Figure 1a compares the cyclic response of loose untreated and treated samples of similar void ratios,  $e$ , also subjected to similar CSR (0.23 to 0.25) under  $p'_0 = 100\text{kPa}$ . It is indicated that the untreated sand experiences much larger strain in fewer loading cycles,  $N$ , than the corresponding treated samples. Whereas the values of  $N$  at  $\varepsilon_{DA} = 1, 2.5$  and  $5\%$  are very close for the untreated sample, for the treated samples with both CS = 6% and 10% there is a distinct difference between  $N$  at  $\varepsilon_{DA} = 2.5$  and  $5\%$ . For the latter samples,  $\varepsilon_{DA}$  increases gradually during cyclic loading. Figures 1b and c show the excess pore water pressure ratio,  $\Delta u/p'_0$ , evolution in time and the stress path in the deviatoric stress,  $q = \sigma'_a - \sigma'_r$ , versus mean effective stress,  $p' = (\sigma'_a + 2\sigma'_r)/3$ , space, respectively, for the untreated sample. As seen for the untreated samples,  $\varepsilon_{DA}$  increases rapidly and complete liquefaction ( $\Delta u/p'_0 = 98\%$ ) is reached at  $\varepsilon_{DA} = 3\%$ . The same pattern of behaviour was also observed at different  $e$  and CSR values.

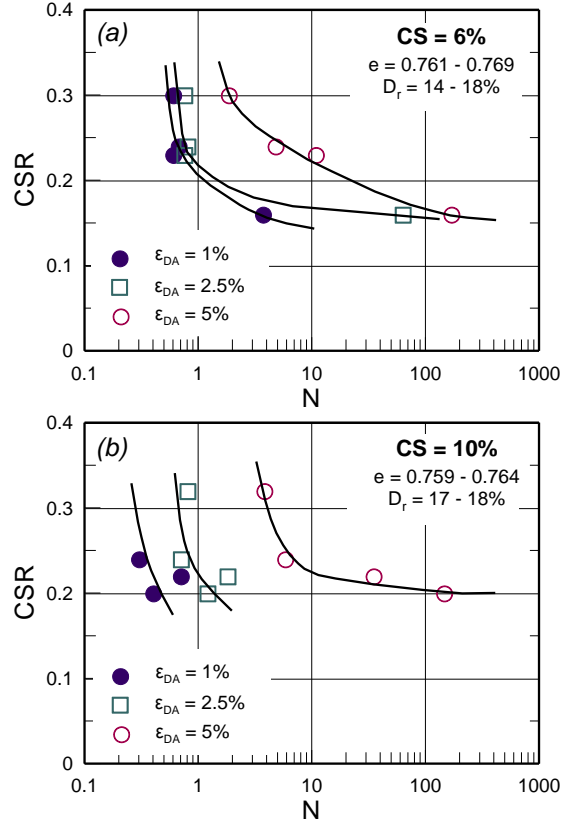
Figure 2 presents for various  $N$  values the CSR required to reach three levels of  $\varepsilon_{DA} = 1, 2.5$  and  $5\%$ , for the treated samples at a loose state with CS = 6% (Figure 2a) and 10% (Figure 2b), under  $p'_0 = 100\text{kPa}$ . The numbers of cycles required to reach  $\varepsilon_{DA} = 1, 2.5$  and  $5\%$  are considerably different from each other for both CS = 6% and 10%.

Figure 3a presents the variation of CSR with number  $N_1$  at  $\varepsilon_{DA} = 5\%$ , for treated and untreated samples at a loose state, at  $p'_0 = 100\text{kPa}$ . There is a remarkable increase of  $N_1$  for treated samples as compared to the corresponding of the untreated. Furthermore, it is shown that the  $N_1$  values for samples with CS = 6% and 10% are very similar with each other at high

CSR values. The same observation holds for treated samples at a medium dense state.



**Figure 1.** (a) Variation of double amplitude axial strain,  $\epsilon_{DA}$  with time,  $t$ , for treated and untreated sands, for  $e = 0.733-0.743$  and  $CSR \approx 0.23$  under  $p'_0 = 100kPa$ . (b) Variation of normalized excess pore water pressure,  $\Delta u/p'_0$ , with time,  $t$ , and (c) deviatoric stress,  $q$ , with mean effective stress,  $p'$ , for the untreated sand of Fig. 1a.



**Figure 2.** Variation of CSR, with number of cycles  $N$ , for treated samples with (a) CS = 6% and (b) 10%, at various values of  $\epsilon_{DA}$ , at  $p'_0 = 100kPa$ .

The variation of  $CRR_{15}$  with  $e$ , for untreated and treated sands at  $p'_0 = 100kPa$ , is presented in Figure 3b. It is shown that treated sands exhibit practically identical  $CRR_{15}$ , irrespectively of the CS concentration, which is at least double the cyclic resistance of untreated sands, under  $p'_0 = 100kPa$ , for the studied range of densities.

### 3.2 Shear stiffness

The small-strain shear modulus,  $G_{max}$ , defined as the linear elastic shear modulus, can be determined from  $V_s$  by the following equation:

$$G_{max} = V_s^2 \cdot \rho \quad (1)$$

where  $\rho$  is total mass density of the soil and it can be expressed by the following empirical equation (Jamiolkowski et al. 1991):

$$G_{\max} = A \cdot p_a^{1-m} \cdot e^n \cdot p'_0{}^m \quad (2)$$

where  $p_a$  is a reference stress, assumed to be 100 kPa, and  $A$ ,  $m$  and  $n$  are parameters dependent on soil type.

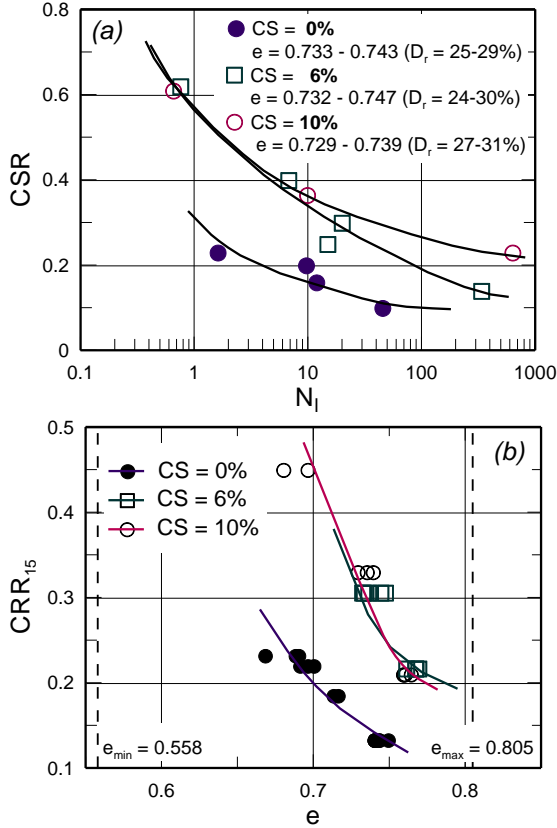


**Figure 3.** Variation of (a) CSR, with number of cycles,  $N_1$ , required for  $\epsilon_{DA} = 5\%$  and (b)  $CRR_{15}$  with void ratio,  $e$ , for treated and untreated samples, at  $p'_0 = 100\text{kPa}$ .

The small-strain shear modulus,  $G_{\max}$ , was estimated from the measured  $V_s$  values in the bender element tests using equation (1). Table 1 lists the values of parameters  $A$ ,  $m$  and  $n$  derived for the untreated and treated sands, according to equation (2). Figure 4 presents the results from the bender element tests. To correct for the effect of density,  $G_{\max}$

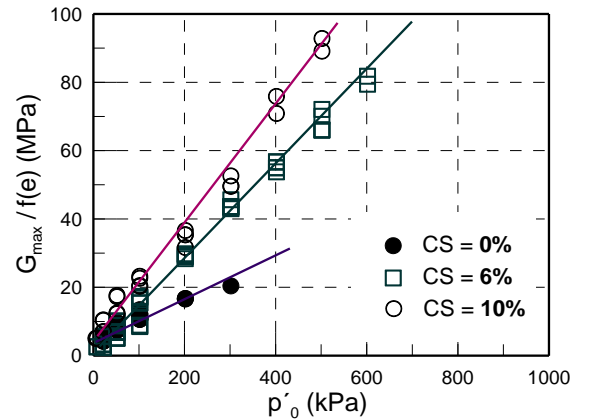
was normalized using the void ratio function,  $f(e) = e^n$ . It is shown that both the presence and concentration of CS have a positive effect on the small-strain shear modulus of treated samples. For the CS concentration used in this work, the increase of normalized small-strain shear modulus of treated samples,  $[G_{\max}/f(e)]_{\text{treated}}$ , over that of the untreated,  $[G_{\max}/f(e)]_{\text{untreated}}$ , increases with both  $p'_0$  and CS, as shown in Figure 5. At CS = 6% and  $p'_0 \leq 50\text{kPa}$ , there is no effect of CS stabilization on the shear stiffness of the sand. At  $p'_0 \geq 100\text{kPa}$ , the treated samples with CS = 10% show 35% higher values of normalized shear stiffness, than the corresponding values of the treated samples with CS = 6%.

Figure 6 presents the correlation of  $CRR_{15}$  with shear wave velocity,  $V_s$ , for treated and untreated sands at  $p'_0 = 100\text{kPa}$ . It is indicated that the rate of increase of  $CRR_{15}$  with  $V_s$  increases with both CS presence and concentration.

**Table 1.** Values of parameters  $A$ ,  $m$  and  $n$  derived from bender element tests.

CS (%)	$A$ ( $10^3$ )	$m$	$n$	( $r^2$ )*
0	381.221	0.545	-6	0.960
6	381.221	0.545	-6.5	0.983
10	381.221	0.545	-5	0.982

\* coefficient of correlation



**Figure 4.** Variation of normalized small-strain shear modulus,  $G_{\max}/f(e)$ , with effective mean stress,  $p'_0$ , for treated and untreated samples.

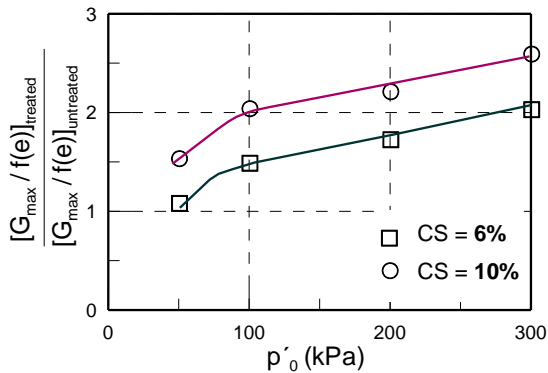


**Figure 5.** Increase of normalized shear stiffness ratio,  $G_{\max} / f(e)$  of treated samples over the corresponding of untreated.

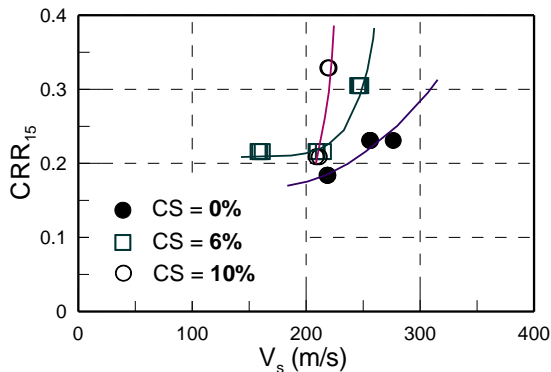


**Figure 6.** Correlation of cyclic resistance ratio,  $CRR_{15}$ , with shear wave velocity,  $V_s$ , at  $p'_0 = 100\text{kPa}$  for treated and untreated samples.

#### 4 CONCLUSIONS

The following conclusions can be drawn from the results of this work on the behaviour of sands stabilized with CS = 6% and 10% and under the range of stresses and densities studied:

- CS stabilization improves significantly both the cyclic resistance and the shear stiffness of the treated samples.
- the treated samples exhibit increased deformation resistance to cyclic loading, as compared to untreated samples which experience much larger  $\epsilon_{DA}$  in fewer cycles.
- treated sands exhibit approximately double the cyclic resistance of untreated sands, irrespectively of CS concentration.

- both the CS presence and concentration have a positive effect on shear stiffness. At a given CS concentration and density, the increase of small-strain shear modulus of the treated samples over that of the untreated, increases with  $p'_0$ .

#### ACKNOWLEDGEMENT

This research has been co-financed by the European Union (European Social Fund–ESF) and Greek national funds through the Operational Program "Education and Lifelong Learning" of the National Strategic Reference Framework (NSRF) - Research Funding Program: Thales.

#### REFERENCES

- Brignoli, E.G.M., Gotti, M. & Stokoe, K.H., II 1996. Measurement of shear waves in laboratory specimens by means of piezoelectric transducers, *Geot. Test. J.*, GTJODJ, ASTM, **4**, 384-397.
- Díaz-Rodríguez, J.A. Antonio-Izarraras, V.M. Bandini, P. & López-Molina, J.A. 2008. Cyclic strength of a natural liquefiable sand stabilized with colloidal silica grout, *Can. Geotech. Journal* **45**, 1345–1355.
- Gallagher, P.M. & Mitchell, J.K. 2002. Influence of colloidal silica grout on liquefaction potential and cyclic undrained behavior of loose sand, *Soil Dynamics and Earthquake Eng.* **22**, 1017-1026.
- Iler, R.K. 1979. *The chemistry of silica: solubility, polymerization, colloid and surface properties and biochemistry*, John Wiley & Sons, New York, NY.
- Kabashima, Y. & Towhata, I. 2000. Improvement of dynamic strength of sand by means of infiltration grouting. *Ground Improvement Techniques, Proceedings, 3<sup>rd</sup> Int. Conf.* Ed.: Pinto, M., 203-208. Singapore.
- Kawaguchi, T., Mitachi, T. & Shibuya, S. 2001. Evaluation of shear wave travel time in laboratory Bender element test. *Proc. Of the 15<sup>th</sup> International Conference on Soil Mechanics and Geotechnical Engineering*, Vol. 1, 155-158. Balkema, Istanbul.
- Ladd, S. 1978. Preparing test specimens using undercompaction, *Geot. Test. J.*, GTJODJ, ASCE, **1**, 16-23.
- Mancuso, C., Simonelli, A.L. & Vinale, F. 1989. Numerical analysis of in situ S-wave measurements, *12<sup>th</sup> ICSMFE, Proceedings*, Vol. 3, 277-280, Rio de Janeiro.
- Mollamahmutoglu, M. & Yilmaz, Y. 2010. Pre- and post-cyclic loading strength of silica grouted sand, *Geot. Engineering* **163** (GE6), 343-348.
- Theopoulos, A. 2009. *A computerized measurement system for analysis of wave characteristics in soil specimen*. M.Sc. thesis, Aristotle University of Thessaloniki, Greece.
- Vranna A.D. & Tika, Th. 2015. The mechanical behaviour of a clean sand stabilized with colloidal silica. *Proceedings, XVI European Conference on Soil Mechanics and Geotechnical Engineering*, Edinburgh, UK, Sept. 13-17.